Title

Palmoplantar keratoderma along with neuromuscular and metabolic phenotypes in Slurp1-deficient mice.

Journal

The Journal of investigative dermatology, 134(6)

ISSN

0022-202X

Authors

Adeyo, Oludotun
Allan, Bernard B
Barnes, Richard H
et al.

Publication Date

2014-06-01

DOI

10.1038/jid.2014.19

Peer reviewed

HHS Public Access

Author manuscript

J Invest Dermatol. Author manuscript; available in PMC 2014 December 01.

Published in final edited form as:

J Invest Dermatol. 2014 June ; 134(6): 1589–1598. doi:10.1038/jid.2014.19.

Palmoplantar keratoderma along with neuromuscular and metabolic phenotypes in *Slurp1*-deficient mice

Oludotun Adeyo[1], **Bernard B. Allan**[5], **Richard H. Barnes II**[1], **Chris N. Goulbourne**[1], **Angelica Tatar**[1], **Yiping Tu**[1], **Lorraine C. Young**[1], **Michael Weinstein**[1], **Peter Tontonoz**[3,4], **Loren G. Fong**[1], **Anne P. Beigneux**[1,†], and **Stephen G. Young**[1,2,†]

[1]Department of Medicine, David Geffen School of Medicine, University of California, Los Angeles, CA 90095

[2]Department of Human Genetics, David Geffen School of Medicine, University of California, Los Angeles, CA 90095

[3]Department of Pathology and Laboratory Medicine, David Geffen School of Medicine, University of California, Los Angeles, CA 90095

[4]Howard Hughes Medical Institute, Genentech, South San Francisco, CA 94080

[5]Department of Molecular Biology, Genentech, South San Francisco, CA 94080

Abstract

Mutations in *SLURP1* cause *mal de Meleda*, a rare palmoplantar keratoderma (PPK). SLURP1 is a secreted protein that is expressed highly in keratinocytes but has also been identified elsewhere (*e.g.*, spinal cord neurons). Here, we examined *Slurp1*-deficient mice ($Slurp1^{-/-}$) created by replacing exon 2 with β-gal and *neo* cassettes. $Slurp1^{-/-}$ mice developed severe PPK characterized by increased keratinocyte proliferation, an accumulation of lipid droplets in the stratum corneum, and a water barrier defect. In addition, $Slurp1^{-/-}$ mice exhibited reduced adiposity, protection from obesity on a high-fat diet, low plasma lipid levels, and a neuromuscular abnormality (hind limb clasping). Initially, it was unclear whether the metabolic and neuromuscular phenotypes were due to *Slurp1* deficiency because we found that the targeted *Slurp1* mutation reduced the expression of several neighboring genes (*e.g., Slurp2, Lypd2*). We therefore created a new line of knockout mice ($Slurp1X^{-/-}$ mice) with a simple nonsense mutation in exon 2. The *Slurp1X* mutation did not reduce the expression of adjacent genes, but $Slurp1X^{-/-}$ mice exhibited all of the phenotypes observed in the original line of knockout mice. Thus, *Slurp1* deficiency in mice elicits metabolic and neuromuscular abnormalities in addition to PPK.

†Correspondence: Anne P. Beigneux or Stephen G. Young, 650 Charles E. Young Dr. South, Los Angeles, CA 90095. Tel: (310) 825-4934; Fax: (310) 206-0865; abeigneux@mednet.ucla.edu, sgyoung@mednet.ucla.edu.

Conflict of interest

The authors have declared that no conflict of interest exists.

Introduction

Mal de Meleda, a severe form of palmoplantar keratoderma (PPK), is caused by mutations in *SLURP1* (Eckl *et al.*, 2003; Fischer *et al.*, 2001; Marrakchi *et al.*, 2003). The disease is very rare and there are relatively few thorough descriptions of disease phenotypes (Charfeddine *et al.*, 2003; Eckl *et al.*, 2003; Fischer *et al.*, 2001; Marrakchi *et al.*, 2003; Oh *et al.*, 2011). Affected patients have thickening of the skin on the palms and soles, occasionally with pseudoainhum formation and autoamputation of digits. The skin of the palms and soles is often malodorous. *Mal de Meleda* patients have two defective *SLURP1* alleles; heterozygous carriers are normal.

The protein that is defective in *Mal de Meleda*, SLURP1, is a member of the "Lymphocyte Antigen 6" (Ly6) protein family. The hallmark of Ly6 proteins is an ~80–amino acid domain containing 10 cysteines, all disulfide-bonded and arranged in a characteristic spacing pattern (Galat *et al.*, 2008; Kieffer *et al.*, 1994). The same motif is found in cobra and viper toxins, many of which target the neuromuscular acetylcholine receptor (Fry *et al.*, 2003; Galat *et al.*, 2008). The majority of mammalian Ly6 proteins are glycosylphosphatidylinositol (GPI)-anchored proteins, but SLURP1 is a secreted protein. SLURP1 is expressed at high levels in keratinocytes, with particularly high levels in the palms and soles (Favre *et al.*, 2007). Because SLURP1 is secreted, it can be found in plasma and urine (Andermann *et al.*, 1999; Mastrangeli *et al.*, 2003). SLURP1 has also been found in rat spinal cord neurons (Moriwaki *et al.*, 2009).

There are many causes of PPK, and nearly all involve defects in structural proteins of keratinocytes (Bowden, 2010; Brooke *et al.*, 2012; Heathcote *et al.*, 2000; Liu *et al.*, 2009; Maestrini *et al.*, 1999; Petrof *et al.*, 2012; Richardson *et al.*, 2006; Xu and Nicholson, 2013). *Mal de Meleda* is unusual in being caused by a secreted protein. Neither SLURP1's interactions with other proteins nor its role in epidermal differentiation are fully understood, but SLURP1 was reported to potentiate acetylcholine signaling through the α-7-nicotinic acetylcholine receptor (α7nAChR) (Chimienti *et al.*, 2003). Subsequent studies suggested that SLURP1 "ligation" to α7nAChR leads to increased acetylcholine signaling, which in turn leads to increased calcium signaling in keratinocytes and effects on kinase expression (Arredondo *et al.*, 2005; Chernyavsky *et al.*, 2010). However, no one has yet tested whether SLURP1 directly interacts with α7nAChR on the surface of cells.

SLURP1 is one of nine Ly6 genes within a ~550-kb segment of human chromosome 8 (chromosome 15 in the mouse). Only one of these genes, *Gpihbp1*, has been studied in depth (Beigneux *et al.*, 2007; Beigneux *et al.*, 2011; Davies *et al.*, 2010; Weinstein *et al.*, 2008). We showed that GPIHBP1, a GPI-anchored protein of endothelial cells, is crucial for plasma triglyceride metabolism; it binds lipoprotein lipase and transports it to the capillary lumen (Beigneux *et al.*, 2007; Davies *et al.*, 2010). Several other genes in this cluster (*e.g.*, *Slurp1*, *Slurp2*, *Ly6d*) are expressed highly in keratinocytes.

Over the past few years, we have begun to investigate the functional relevance of "Ly6 genes" near *Gpihbp1*. We had dual motivations. One was to investigate the *in vivo* relevance of Ly6 proteins in keratinocytes, and a second was to determine if other Ly6 genes, aside

from *Gpihbp1*, were relevant to metabolism. We began our studies with *Slurp1* because there were no published reports of *Slurp1* knockout mice and we were intrigued by reports that SLURP1 is a small secreted protein that can be found in the plasma. Our studies yielded fresh insights into SLURP1 function in the skin and uncovered completely unexpected consequences of *Slurp1* deficiency in mice.

Results

Slurp1 knockout mice, created by replacing exon 2 with *neo* and *lacZ* cassettes (Fig. S1), appeared normal at birth but developed PPK by 6 weeks of age (Fig. 1 A–C). By H&E staining, the epidermis in *Slurp1*$^{-/-}$ paw skin was thickened and the stratum granulosum was poorly demarcated (Fig. 1 B). No inflammatory infiltrates were present. The stratum corneum contained abundant lipid droplets, as judged by H&E staining, BODIPY staining, and electron microscopy (Fig. 1 C–E). Lamellar bodies were present in stratum granulosum keratinocytes in both wild-type and *Slurp1*$^{-/-}$ mice, as determined by electron microscopy (Fig. S 2), but whether this technique is capable of picking up subtle differences in the efficiency of lamellar body secretion is uncertain. BrdU incorporation into keratinocytes of paw skin in *Slurp1*$^{-/-}$ mice was markedly increased (Fig. 1 F). Aside from the paw, the skin and hair of *Slurp1*$^{-/-}$ mice were normal, both grossly and by routine histology (Fig. S3). The gastrointestinal tract, bronchial epithelium, and lungs of *Slurp1*$^{-/-}$ mice were histologically normal. Humans with *mal de Meleda* have been reported to have perivascular lymphocytic infiltrates and perioral involvment (Bouadjar *et al.*, 2000; Nath *et al.*, 2012), but these features were not present in *Slurp1*$^{-/-}$ mice. *Slurp1*$^{+/-}$ mice were indistinguishable from wild-type mice.

SLURP1 could be documented in the paw skin of wild-type mice but was absent in *Slurp1*$^{-/-}$ mice (Fig. 2 A). Our *mouse* SLURP1 antibodies were not useful for immunohistochemistry (and the *lacZ* cassette was not expressed), making it impossible to visualize SLURP1 expression in mouse skin. However, a *human* SLURP1-specific antibody detected SLURP1 in the suprabasal layers (including the spinous and granular layers) of human skin (Fig. 2 C), confirming earlier reports (Favre *et al.*, 2007; Mastrangeli *et al.*, 2003).

Because SLURP1 is expressed in the stratum granulosum of human skin (the layer that creates the water barrier) and also because of the accumulation of lipids in the stratum corneum of *Slurp1*$^{-/-}$ mice, we assessed transepidermal water loss in *Slurp1*$^{-/-}$ and wild-type mice. Water loss from the paw skin of *Slurp1*$^{-/-}$ mice was significantly greater than in wild-type mice, but water loss from the skin on the ear and back was similar in the two groups of mice (Fig. 3).

Slurp1$^{-/-}$ mice exhibited a neuromuscular phenotype: they clasped their hind limbs when picked up by the tail (a phenotype often observed in the setting of central nervous system disease, myopathy, or peripheral neuropathy) (Dequen *et al.*, 2010; Hayward *et al.*, 2008; Lalonde and Strazielle, 2011) (Fig. 4 A–B). The sciatic nerve of *Slurp1*$^{-/-}$ mice was normal by routine histology and by electron microscopy (Fig. S4), and no pathology was observed

in the cerebral cortex or cerebellum. Serum chemistries in *Slurp1*$^{-/-}$ mice, including creatine phosphokinase levels, were within normal limits.

Slurp1$^{-/-}$ mice also exhibited metabolic phenotypes; they had reduced body weight and adiposity on a chow diet, despite consuming more food (Fig. 4 C–E). They were also protected from obesity on a high-fat diet (Fig. 4 F–G). The plasma levels of triglycerides, cholesterol, insulin, and leptin were lower in *Slurp1*$^{-/-}$ mice than in wild-type littermate controls (Fig. 5 A–C). Metabolic cage studies showed that mean O_2 consumption and CO_2 production were higher in *Slurp1*$^{-/-}$ mice; the respiratory quotient was higher in *Slurp1*$^{-/-}$ mice during the dark phase (Fig. 5 D–F and Fig. S5 A–C). Surprisingly, physical activity in *Slurp1*$^{-/-}$ mice was lower, as judged by laser beam breaks in metabolic cages (Fig. 5 G and Fig. S5 D). We considered the possibility that hyperventilation might contribute to increased oxygen consumption, but this appeared unlikely because the serum bicarbonate levels were within normal limits (13.6 ± 0.56 mEq/L in wild-type mice and 11.55 ± 2.30 mEq/L in *Slurp1*$^{-/-}$ mice). It is conceivable that increased grooming in *Slurp1*$^{-/-}$ mice (a form of activity that might not lead to laser beams breaks) could account for the increased oxygen consumption, but studies of grooming behavior in *Slurp1*$^{-/-}$ mice with continuous video monitoring provided no evidence that this was the case.

We suspected that the metabolic abnormalities would be accompanied by gene-expression perturbations in peripheral tissues. Hormone-sensitive lipase (HSL) and adipose triglyceride lipase (ATGL) were increased in brown and white adipose tissue (Fig. S6). Also, PGC-1α expression was higher in the soleus muscle, liver, and heart of *Slurp1*$^{-/-}$ mice (Fig. S6), and the expression of the fatty acid transport protein (FATP-1), which plays an important role in facilitating mitochondrial fatty acid oxidation (Sebastian *et al.*, 2009; Wiczer and Bernlohr, 2009), was increased in the quadriceps, soleus, brown adipose tissue, and white adipose tissue (Fig. S6). UCP1 expression in brown adipose tissue was similar in *Slurp1*$^{-/-}$ and wild-type mice (Fig. S6).

Because the neuromuscular and metabolic phenotypes were unexpected, we worried that the targeted *Slurp1* mutation, which involved insertions of β-gal and *neo* cassettes, might have influenced the expression of neighboring genes (Olson *et al.*, 1996). Indeed, the expression of two Ly6 genes adjacent to *Slurp1* (*Slurp2* and *Lypd2)* was reduced by 60–75% in *Slurp1*$^{-/-}$ mice, while the expression of a more distant Ly6 family member, *Ly6d*, was unaffected (Fig. S7 A). Perturbed expression of *Slurp2* and *Lypd2* was also present in *Slurp1*$^{+/-}$ mice, where the paw skin is normal, implying that the effects of the targeted *Slurp1* mutation on neighboring genes were due to effects on chromatin structure and not an indirect consequence of PPK.

The fact that the *Slurp1* mutation lowered the expression of nearby genes suggested that the “non-PPK” phenotypes in *Slurp1*$^{-/-}$ mice might be due to altered expression of neighboring genes rather than to SLURP1 deficiency. To address that possibility, we created new *Slurp1* knockout mice harboring only a simple nonsense mutation (Fig. S7 B–D). This allele, designated *Slurp1X*, did not lower the expression of adjacent genes (Fig. S7 E). Nevertheless, homozygous knockout mice (*Slurp1X*$^{-/-}$) exhibited all of the phenotypes found in the original *Slurp1*$^{-/-}$ mice (PPK, reduced body weight, hind limb clasping) (Fig.

6). In fact, the neuromuscular abnormalities were more striking in *Slurp1X*$^{-/-}$ mice; aside from hind limb clasping, they dragged their hind limbs and tail by 4 months of age (Supplementary Movies 1 and 2).

Discussion

In the current study, we investigated *Slurp1* knockout mice, fully expecting to encounter PPK. That expectation was fulfilled, but we also found neuromuscular and metabolic/body weight abnormalities. Initially, whether SLURP1 deficiency caused the "non-PPK" phenotypes seemed uncertain because the targeted mutation, which involved insertions of β-gal and *neo* cassettes, lowered the expression of nearby genes. However, a new line of *Slurp1* knockout mice harboring a simple nonsense mutation—and where the expression of surrounding genes was normal—displayed the same neuromuscular and metabolic phenotypes, leaving no doubt that the "non-PPK" phenotypes were *bona fide* features of SLURP1 deficiency. We considered the possibility that the unexpected phenotypes could be due to "passenger genes" segregating with *Slurp1* (Smithies and Maeda, 1995), but this explanation is highly unlikely because neuromuscular and body weight phenotypes are absent in chow-fed knockout mice for nearby Ly6 genes (*Lynx1* and *Gpihbp1*) (Beigneux *et al.*, 2007; Ibanez-Tallon *et al.*, 2002; Miwa *et al.*, 2006; Weinstein *et al.*, 2012; Weinstein *et al.*, 2010a; Weinstein *et al.*, 2010b).

Why a deficiency of SLURP1, a secreted Ly6 protein, causes PPK is uncertain, but one possibility, suggested by Fischer *et al.* (Fischer *et al.*, 2001), is that SLURP1 is a ligand for a cell-surface receptor on keratinocytes. Chimienti *et al.* (Chimienti *et al.*, 2003) reported that SLURP1 potentiates calcium flow mediated by the α-7 nicotinic acetylcholine receptor (α7nAChR). Also, Arredondo et al. (Arredondo *et al.*, 2005) reported that SLURP1 competitively inhibits binding of small-molecule ligands to that receptor. The involvement of acetylcholine receptors in the pathogenesis of *mal de Meleda* is potentially attractive because acetylcholine signaling is thought to be important in multiple aspects of keratinocyte biology and because the three-fingered structure of SLURP1 resembles cobra toxins that bind to acetylcholine receptors at the neuromuscular junction (Andermann *et al.*, 1999; Fischer *et al.*, 2001; Kini, 2002). Also, a "SLURP1–acetylcholine connection" could potentially be relevant to both the skin and neuromuscular phenotypes of *Slurp1*$^{-/-}$ mice. At this point, what is needed is firm evidence for specific protein–protein interactions between SLURP1 and acetylcholine receptors. Thus far, we have not been successful in documenting SLURP1 binding to α7nAChR on the surface of CHO-K1 cells using the same cell-based binding assays that have been used extensively to document the binding of a protein ligand to GPIHBP1 (an Ly6 protein that is structurally related to SLURP1) (Beigneux *et al.*, 2011; Beigneux *et al.*, 2009; Franssen *et al.*, 2010; Olafsen *et al.*, 2010; Voss *et al.*, 2011). However, it is possible that our cell-based binding assays were not sufficiently sensitive to detect SLURP1–α7nAChR interactions. In addition, we have not yet tested the possibility that SLURP1 might bind to other acetylcholine receptors. In any case, we believe that a "SLURP1–acetylcholine receptor connection" is an attractive concept and deserves further study. We also believe that it is important to be open to other possibilities for SLURP1 function. One is that SLURP1 binds to and modifies the function of structural proteins already implicated in the pathogenesis of PPK, for example demosomal proteins (Bowden,

2010; Brooke *et al.*, 2012; Liu *et al.*, 2009; Petrof *et al.*, 2012; Richardson *et al.*, 2006) or connexin 26, a gap junction protein (Heathcote *et al.*, 2000; Maestrini *et al.*, 1999; Xu and Nicholson, 2013). The idea that SLURP1 might affect cell–cell junctions has been raised previously (Fischer *et al.*, 2001) and is not farfetched because another Ly6 protein, LY6D, is present in desmosomes (Brakenhoff *et al.*, 1995; Fischer *et al.*, 2001). Also, *Drosophila* Ly6 proteins are crucial for the septate junctions that cement epithelial cells together (Hijazi *et al.*, 2011; Hijazi *et al.*, 2009; Kim and Marques, 2012; Nilton *et al.*, 2010).

The mechanism by which SLURP1 deficiency elicits the neuromuscular findings is unknown. One possibility is that SLURP1 plays a role in peripheral nerves, perhaps (as suggested by Moriwaki *et al.* (Moriwaki *et al.*, 2009)) by acting as a neurotransmitter. Improved antibody reagents will be required to investigate this possibility. A more speculative idea relates to the possible involvement of SLURP1 in cell–cell junctions in peripheral nerves (Banerjee *et al.*, 2006). Genetic manipulations of axo-glial septate junction proteins in mice alter nerve conduction and elicit the same hind limb clasping phenotype found in *Slurp1*$^{-/-}$ mice (Cifuentes-Diaz *et al.*, 2011; Lee *et al.*, 2013). No one has yet reported neuropathy in *mal de Meleda* patients, but we would not be surprised if sophisticated testing were to uncover subtle abnormalities.

SLURP1 deficiency reduced body weight and adiposity, increased oxygen consumption, and lowered plasma lipid and insulin levels. The same phenotypes have been observed in mice lacking stearoyl-CoA desaturase-1 (SCD1), which is required for lipid synthesis and the formation of the epidermal water barrier (Binczek *et al.*, 2007; Sampath *et al.*, 2009). *Scd1* knockout mice display increased evaporative water loss, leading to loss of body heat and increased energy expenditure (Binczek *et al.*, 2007). We doubt that the same mechanism applies in *Slurp1*$^{-/-}$ mice. First, the water barrier defect in *Slurp1*$^{-/-}$ mice is confined to the paw, and it seems unlikely that water loss from this tiny area of skin would explain the striking metabolic abnormalities. Second, *Slurp1* deficiency did not increase expression of thermogenic genes in brown adipose tissue. Third, reduced body weight is not a general feature of PPK; *grainy head-like 1* knockout mice have severe PPK but no alterations in body weight (Wilanowski *et al.*, 2008).

While body weight and adiposity abnormalities in SLURP1-deficient mice are profound, the underlying mechanisms are not clear. It is tempting to speculate that SLURP1, a secreted peptide found in the plasma, may act directly or indirectly to increase fuel utilization in metabolically active tissues. We did observe increased expression of HSL and ATGL (genes involved in intracellular lipolysis) in adipose tissue of *Slurp1*$^{-/-}$ mice; we also found increased *Pgc1*α and *Fatp1* expression in multiple tissues of *Slurp1*$^{-/-}$ mice.

We found an accumulation of neutral lipid droplets in the stratum corneum of paw skin of *Slurp1*$^{-/-}$ mice. In earlier studies, lipid droplets were observed in the fingernails of *mal de Meleda* patients (Salamon, 1986; Salamon *et al.*, 1984), and higher triglyceride levels were also found in the epidermis of several *mal de Meleda* patients (Kuster *et al.*, 2003). The increased numbers of lipid droplets in the stratum corneum are likely due to impaired hydrolysis of triglycerides, a process that is essential for the formation of acylceramides and the epidermal water barrier (Elias *et al.*, 2008). A similar accumulation of neutral lipid

droplets in the stratum corneum is found in neutral lipid storage disease due to CGI-58 deficiency (Demerjian *et al.*, 2006), where triglyceride hydrolysis is clearly impaired (Radner *et al.*, 2011; Radner *et al.*, 2010; Ujihara *et al.*, 2010). We did not find reduced transcript levels for CGI-58, ATGL, triglyceride hydrolase K, or triglyceride hydrolase N in paw skin of *Slurp1*$^{-/-}$ mice (not shown). Nevertheless, it seems likely that SLURP1 deficiency influences the efficiency of triglyceride hydrolysis in keratinocytes, perhaps indirectly as a consequence of altered keratinocyte proliferation or differentiation.

Our findings are relevant to clinical dermatology. The discovery of a defective water barrier in SLURP1-deficient skin, along with increased neutral lipids in the stratum corneum, could help to explain malodorous skin in *mal de Meleda* (Oh *et al.*, 2011). Leakage of interstitial fluids into the stratum corneum along with the accumulation of triglyceride droplets would favor the growth of microorganisms, and bacterial lipases are known to release malodorous aldehydes, alcohols, and ketones (Chung and Seok, 2012). Also, our studies reinforce the fact that genetic defects causing PPK can be accompanied by “non-skin” disease phenotypes. Other genetic defects causing PPK are associated with deafness, right ventricular dysplasia, and central nervous system disease (Brooke *et al.*, 2012; Heathcote *et al.*, 2000; Petrof *et al.*, 2012; Xu and Nicholson, 2013). In the current studies, we found that SLURP1 deficiency in the mouse leads to neuromuscular and body weight abnormalities.

Materials and Methods

Slurp1-deficient mice

Slurp1$^{-/-}$ mice were obtained from Lexicon. The *Slurp1* knockout allele was detected by PCR genotyping as described in the Supplementary Methods. *Slurp1X* mice were created by introducing a premature stop codon into exon 2 (N35X), as described in the Supplementary Methods and Supplementary Figure 6. All mice had a mixed genetic background (<10% 129/Sv and >90% C57BL/6). Unless otherwise specified, the mice were fed a chow diet (LabDiet No. 5001, Purina) and housed in a barrier facility with a 12-h light/dark cycle. All studies were approved by UCLA’s Animal Research Committee.

Histology and immunofluorescence microscopy

Skin biopsies were fixed overnight in 10% formalin, embedded in paraffin, sectioned, and stained with hematoxylin and eosin. For immunohistochemistry, cultured cells and frozen sections of human skin were fixed in methanol. The cells and tissues were blocked with 10% donkey serum and incubated with primary antibodies at 4°C overnight. Antibodies included a goat polyclonal antibody against the S-protein tag (Abcam; 1:500), a mouse antiserum against human SLURP1 (Novus Biologicals; 1:100), a rat monoclonal antibody against BrdU (Abcam; 1:200), or an Alexa 568-labeled mouse monoclonal antibody against cytokeratin 14 (Abcam; 1:500). Secondary antibodies included an Alexa 568–conjugated donkey anti-goat IgG (Invitrogen; 1:800), an Alexa 488–conjugated donkey anti-mouse IgG (Invitrogen; 1:800), and an Alexa 488–conjugated donkey anti-rat IgG (Invitrogen; 1:200). DNA was visualized with DAPI. Microscopy was performed with an Axiovert 200M microscope.

Western Blotting

Proteins from tissue or cell culture extracts (25 μg) were size-fractionated on a 12% Bis-Tris SDS-polyacrylamide gel and then transferred to nitrocellulose membranes. Antibodies included a mouse monoclonal antibody against β-actin (1:500) (Abcam, Cambridge, MA); a rabbit antiserum against a SLURP1 peptide (CKTVLETVEAAFPFNHSPMVTRS) (5 μg/ml; an IRdye800-conjugated donkey anti-rabbit and donkey anti-mouse IgG (1:2,000) (Li-Cor, Lincoln, NE). Antibody binding was detected with an Odyssey infrared scanner (Li-Cor).

Quantification of Transepidermal Water Loss

Transepidermal water loss (TEWL) measurements on the skin of the back, rear paws, and ear were recorded at room temperature on age- and sex-matched wild-type and *Slurp1*$^{-/-}$ mice (n = 6/group) with an RG1 evaporimeter (cyberDERM) equipped with a 0.3-mm circular adaptor. The hair on a small portion of the back was shaved with a clipper before TEWL measurements were performed.

Body Weight/Metabolic Phenotypes

Body weights of male and female mice were recorded weekly from 4 to 15 weeks of age, and measurements of adiposity were made by NMR (Weinstein *et al.*, 2010a). Measurements of oxygen consumption and respiratory quotient were performed using sealed metabolic cages (Oxymax, Columbus Instruments) (Weinstein *et al.*, 2012). Sensors attached to the sealed chamber measured oxygen and carbon dioxide concentrations, and physical activity was assessed by the number of laser beam breaks. Data was collected and analyzed with Oxymax/CLAMS software. All metabolic cage studies were performed using male mice.

Supplementary Material

Refer to Web version on PubMed Central for supplementary material.

Acknowledgments

This work was supported by P01 HL090553 (SGY), an American Heart Association (AHA) Grant-in-Aid (APB), and AHA postdoctoral fellowship awards (CG).

Abbreviations

PPK	palmoplantar keratoderma
Ly6	lymphocyte antigen 6
GPIHBP1	glycosylphosphatidylinositol-anchored high-density lipoprotein binding protein 1

References

1. Andermann K, Wattler F, Wattler S, Heine G, Meyer M, Forssmann WG, et al. Structural and phylogenetic characterization of human SLURP-1, the first secreted mammalian member of the Ly-6/uPAR protein superfamily. Protein Sci. 1999; 8:810–819. [PubMed: 10211827]
2. Arredondo J, Chernyavsky AI, Webber RJ, Grando SA. Biological effects of SLURP-1 on human keratinocytes. J Invest Dermatol. 2005; 125:1236–1241. [PubMed: 16354194]
3. Banerjee S, Sousa AD, Bhat MA. Organization and function of septate junctions: an evolutionary perspective. Cell biochemistry and biophysics. 2006; 46:65–77. [PubMed: 16943624]
4. Beigneux AP, Davies B, Gin P, Weinstein MM, Farber E, Qiao X, et al. Glycosylphosphatidylinositol-anchored high density lipoprotein–binding protein 1 plays a critical role in the lipolytic processing of chylomicrons. Cell Metab. 2007; 5:279–291. [PubMed: 17403372]
5. Beigneux AP, Davies BS, Tat S, Chen J, Gin P, Voss CV, et al. Assessing the role of the glycosylphosphatidylinositol-anchored high density lipoprotein-binding protein 1 (GPIHBP1) three-finger domain in binding lipoprotein lipase. J Biol Chem. 2011; 286:19735–19743. [PubMed: 21478160]
6. Beigneux AP, Gin P, Davies BS, Weinstein MM, Bensadoun A, Ryan RO, et al. Glycosylation of Asn-76 in mouse GPIHBP1 is critical for its appearance on the cell surface and the binding of chylomicrons and lipoprotein lipase. J Lipid Res. 2008; 49:1312–1321. [PubMed: 18340083]
7. Beigneux AP, Gin P, Davies BSJ, Weinstein MM, Bensadoun A, Fong LG, et al. Highly conserved cysteines within the Ly6 domain of GPIHBP1 are crucial for the binding of lipoprotein lipase. J Biol Chem. 2009; 284:30240–30247. [PubMed: 19726683]
8. Binczek E, Jenke B, Holz B, Gunter RH, Thevis M, Stoffel W. Obesity resistance of the stearoyl-CoA desaturase-deficient (*scd1*$^{-/-}$) mouse results from disruption of the epidermal lipid barrier and adaptive thermoregulation. Biological chemistry. 2007; 388:405–418. [PubMed: 17391062]
9. Bouadjar B, Benmazouzia S, Prud'homme JF, Cure S, Fischer J. Clinical and genetic studies of 3 large, consanguineous, Algerian families with Mal de Meleda. Archives of dermatology. 2000; 136:1247–1252. [PubMed: 11030771]
10. Bowden PE. Mutations in a keratin 6 isomer (K6c) cause a type of focal palmoplantar keratoderma. The Journal of investigative dermatology. 2010; 130:336–338. [PubMed: 20081885]
11. Brakenhoff RH, Gerretsen M, Knippels EM, van Dijk M, van Essen H, Weghuis DO, et al. The human E48 antigen, highly homologous to the murine Ly-6 antigen ThB, is a GPI-anchored molecule apparently involved in keratinocyte cell-cell adhesion. J Cell Biol. 1995; 129:1677–1689. [PubMed: 7790363]
12. Brooke MA, Nitoiu D, Kelsell DP. Cell-cell connectivity: desmosomes and disease. The Journal of pathology. 2012; 226:158–171. [PubMed: 21989576]
13. Charfeddine C, Mokni M, Ben Mousli R, Elkares R, Bouchlaka C, Boubaker S, et al. A novel missense mutation in the gene encoding SLURP-1 in patients with Mal de Meleda from northern Tunisia. Br J Dermatol. 2003; 149:1108–1115. [PubMed: 14674887]
14. Chernyavsky AI, Arredondo J, Galitovskiy V, Qian J, Grando SA. Upregulation of nuclear factor-kappaB expression by SLURP-1 is mediated by alpha7-nicotinic acetylcholine receptor and involves both ionic events and activation of protein kinases. Am J Physiol Cell Physiol. 2010; 299:C903–C911. [PubMed: 20660165]
15. Chimienti F, Hogg RC, Plantard L, Lehmann C, Brakch N, Fischer J, et al. Identification of SLURP-1 as an epidermal neuromodulator explains the clinical phenotype of Mal de Meleda. Hum Mol Genet. 2003; 12:3017–3024. [PubMed: 14506129]
16. Chung H, Seok H. Populations of malodor-forming bacteria and identification of volatile components in triolein-soiled cotton fabric. Fibers and Polymers. 2012; 13:740–747.
17. Cifuentes-Diaz C, Chareyre F, Garcia M, Devaux J, Carnaud M, Levasseur G, et al. Protein 4.1B contributes to the organization of peripheral myelinated axons. PLoS One. 2011; 6:e25043. [PubMed: 21966409]

18. Davies BSJ, Beigneux AP, Barnes RH II, Tu Y, Gin P, Weinstein MM, et al. GPIHBP1 is responsible for the entry of lipoprotein lipase into capillaries. Cell Metab. 2010; 12:42–52. [PubMed: 20620994]
19. Demerjian M, Crumrine DA, Milstone LM, Williams ML, Elias PM. Barrier dysfunction and pathogenesis of neutral lipid storage disease with ichthyosis (Chanarin-Dorfman syndrome). The Journal of investigative dermatology. 2006; 126:2032–2038. [PubMed: 16741516]
20. Dequen F, Filali M, Lariviere RC, Perrot R, Hisanaga S, Julien JP. Reversal of neuropathy phenotypes in conditional mouse model of Charcot-Marie-Tooth disease type 2E. Hum Mol Genet. 2010; 19:2616–2629. [PubMed: 20421365]
21. Eckl KM, Stevens HP, Lestringant GG, Westenberger-Treumann M, Traupe H, Hinz B, et al. Mal de Meleda (MDM) caused by mutations in the gene for SLURP-1 in patients from Germany, Turkey, Palestine, and the United Arab Emirates. Hum Genet. 2003; 112:50–56. [PubMed: 12483299]
22. Elias PM, Williams ML, Holleran WM, Jiang YJ, Schmuth M. Pathogenesis of permeability barrier abnormalities in the ichthyoses: inherited disorders of lipid metabolism. J Lipid Res. 2008; 49:697–714. [PubMed: 18245815]
23. Favre B, Plantard L, Aeschbach L, Brakch N, Christen-Zaech S, de Viragh PA, et al. SLURP1 is a late marker of epidermal differentiation and is absent in Mal de Meleda. J Invest Dermatol. 2007; 127:301–308. [PubMed: 17008884]
24. Fischer J, Bouadjar B, Heilig R, Huber M, Lefevre C, Jobard F, et al. Mutations in the gene encoding SLURP-1 in Mal de Meleda. Hum Mol Genet. 2001; 10:875–880. [PubMed: 11285253]
25. Franssen R, Young SG, Peelman F, Hertecant J, Sierts JA, Schimmel AWM, et al. Chylomicronemia with low postheparin lipoprotein lipase levels in the setting of GPIHBP1 defects. Circ Cardiovasc Genet. 2010; 3:169–178. [PubMed: 20124439]
26. Fry BG, Wuster W, Kini RM, Brusic V, Khan A, Venkataraman D, et al. Molecular evolution and phylogeny of elapid snake venom three-finger toxins. J Mol Evol. 2003; 57:110–129. [PubMed: 12962311]
27. Galat A, Gross G, Drevet P, Sato A, Menez A. Conserved structural determinants in three-fingered protein domains. FEBS J. 2008; 275:3207–3225. [PubMed: 18485004]
28. Hayward LJ, Kim JS, Lee MY, Zhou H, Kim JW, Misra K, et al. Targeted mutation of mouse skeletal muscle sodium channel produces myotonia and potassium-sensitive weakness. J Clin Invest. 2008; 118:1437–1449. [PubMed: 18317596]
29. Heathcote K, Syrris P, Carter ND, Patton MA. A connexin 26 mutation causes a syndrome of sensorineural hearing loss and palmoplantar hyperkeratosis (MIM 148350). J Med Genet. 2000; 37:50–51. [PubMed: 10633135]
30. Hijazi A, Haenlin M, Waltzer L, Roch F. The Ly6 protein coiled is required for septate junction and blood brain barrier organisation in *Drosophila* . PLoS One. 2011; 6:e17763. [PubMed: 21423573]
31. Hijazi A, Masson W, Auge B, Waltzer L, Haenlin M, Roch F. boudin is required for septate junction organisation in *Drosophila* and codes for a diffusible protein of the Ly6 superfamily. Development. 2009; 136:2199–2209. [PubMed: 19502482]
32. Ibanez-Tallon I, Miwa JM, Wang HL, Adams NC, Crabtree GW, Sine SM, et al. Novel modulation of neuronal nicotinic acetylcholine receptors by association with the endogenous prototoxin lynx1. Neuron. 2002; 33:893–903. [PubMed: 11906696]
33. Kieffer B, Driscoll PC, Campbell ID, Willis AC, van der Merwe PA, Davis SJ. Three-dimensional solution structure of the extracellular region of the complement regulatory protein CD59, a new cell-surface protein domain related to snake venom neurotoxins. Biochemistry. 1994; 33:4471–4482. [PubMed: 7512825]
34. Kim NC, Marques G. The Ly6 neurotoxin-like molecule target of wit regulates spontaneous neurotransmitter release at the developing neuromuscular junction in *Drosophila* . Developmental neurobiology. 2012; 72:1541–1558. [PubMed: 22467519]
35. Kini RM. Molecular moulds with multiple missions: functional sites in three-finger toxins. Clinical and experimental pharmacology & physiology. 2002; 29:815–822. [PubMed: 12165048]

36. Kuster W, Melnik B, Traupe H, Hamm H. Lipid composition of outer stratum corneum in hereditary palmoplantar keratodermas. Dermatology. 2003; 206:131–135. [PubMed: 12592080]
37. Lalonde R, Strazielle C. Brain regions and genes affecting limb-clasping responses. Brain research reviews. 2011; 67:252–259. [PubMed: 21356243]
38. Lee SM, Sha D, Mohammed AA, Asress S, Glass JD, Chin LS, et al. Motor and sensory neuropathy due to myelin infolding and paranodal damage in a transgenic mouse model of Charcot-Marie-Tooth disease type 1C. Hum Mol Genet. 2013; 22:1755–1770. [PubMed: 23359569]
39. Liu XP, Ling J, Xiong H, Shi XL, Sun X, Pan Q, et al. Mutation L437P in the 2B domain of keratin 1 causes diffuse palmoplantar keratoderma in a Chinese pedigree. Journal of the European Academy of Dermatology and Venereology : JEADV. 2009; 23:1079–1082. [PubMed: 19470048]
40. Maestrini E, Korge BP, Ocana-Sierra J, Calzolari E, Cambiaghi S, Scudder PM, et al. A missense mutation in connexin26, D66H, causes mutilating keratoderma with sensorineural deafness (Vohwinkel's syndrome) in three unrelated families. Hum Mol Genet. 1999; 8:1237–1243. [PubMed: 10369869]
41. Marrakchi S, Audebert S, Bouadjar B, Has C, Lefevre C, Munro C, et al. Novel mutations in the gene encoding secreted lymphocyte antigen-6/urokinase-type plasminogen activator receptor-related protein-1 (SLURP-1) and description of five ancestral haplotypes in patients with Mal de Meleda. The Journal of investigative dermatology. 2003; 120:351–355. [PubMed: 12603845]
42. Mastrangeli R, Donini S, Kelton CA, He C, Bressan A, Milazzo F, et al. ARS Component B: structural characterization, tissue expression and regulation of the gene and protein (SLURP-1) associated with Mal de Meleda. European journal of dermatology : EJD. 2003; 13:560–570. [PubMed: 14721776]
43. Miwa JM, Stevens TR, King SL, Caldarone BJ, Ibanez-Tallon I, Xiao C, et al. The prototoxin lynx1 acts on nicotinic acetylcholine receptors to balance neuronal activity and survival in vivo. Neuron. 2006; 51:587–600. [PubMed: 16950157]
44. Moriwaki Y, Watanabe Y, Shinagawa T, Kai M, Miyazawa M, Okuda T, et al. Primary sensory neuronal expression of SLURP-1, an endogenous nicotinic acetylcholine receptor ligand. Neurosci Res. 2009; 64:403–412. [PubMed: 19409425]
45. Nath AK, Chaudhuri S, Thappa DM. Mal de meleda with lip involvement: a report of two cases. Indian journal of dermatology. 2012; 57:390–393. [PubMed: 23112362]
46. Nilton A, Oshima K, Zare F, Byri S, Nannmark U, Nyberg KG, et al. Crooked, coiled and crimpled are three Ly6-like proteins required for proper localization of septate junction components. Development. 2010; 137:2427–2437. [PubMed: 20570942]
47. Oh YJ, Lee HE, Ko JY, Ro YS, Yu HJ. A Sporadic Case of Mal de Meleda Caused by Gene Mutation in SLURP-1 in Korea. Annals of dermatology. 2011; 23:396–399. [PubMed: 21909218]
48. Olafsen T, Young SG, Davies BS, Beigneux AP, Kenanova VE, Voss C, et al. Unexpected expression pattern for glycosylphosphatidylinositol-anchored HDL-binding protein 1 (GPIHBP1) in mouse tissues revealed by positron emission tomography scanning. J Biol Chem. 2010; 285:39239–39248. [PubMed: 20889497]
49. Olson EN, Arnold H-H, Rigby PWJ, Wold BJ. Know your neighbors: Three phenotypes in null mutants of the myogenic bHLH gene *MRF4* . Cell. 1996; 85:1–4. [PubMed: 8620528]
50. Petrof G, Mellerio JE, McGrath JA. Desmosomal genodermatoses. The British journal of dermatology. 2012; 166:36–45. [PubMed: 21929534]
51. Radner FP, Grond S, Haemmerle G, Lass A, Zechner R. Fat in the skin: Triacylglycerol metabolism in keratinocytes and its role in the development of neutral lipid storage disease. Dermato-endocrinology. 2011; 3:77–83. [PubMed: 21695016]
52. Radner FP, Streith IE, Schoiswohl G, Schweiger M, Kumari M, Eichmann TO, et al. Growth retardation, impaired triacylglycerol catabolism, hepatic steatosis, and lethal skin barrier defect in mice lacking comparative gene identification-58 (CGI-58). J Biol Chem. 2010; 285:7300–7311. [PubMed: 20023287]
53. Richardson ES, Lee JB, Hyde PH, Richard G. A novel mutation and large size polymorphism affecting the V2 domain of keratin 1 in an African-American family with severe, diffuse

palmoplantar keratoderma of the ichthyosis hystrix Curth-Macklin type. The Journal of investigative dermatology. 2006; 126:79–84. [PubMed: 16417221]

54. Salamon T. Sudan-IV-positive material in fingernails of patient affected with mal de Meleda. Dermatologica. 1986; 173:199–200. [PubMed: 3770264]
55. Salamon T, Plavsic B, Nikulin A. Electron microscopic study of fingernails in the disease of Mljet (Mal de Meleda). Acta dermato-venereologica. 1984; 64:302–307. [PubMed: 6209887]
56. Sampath H, Flowers MT, Liu X, Paton CM, Sullivan R, Chu K, et al. Skin-specific deletion of stearoyl-CoA desaturase-1 alters skin lipid composition and protects mice from high fat diet-induced obesity. J Biol Chem. 2009; 284:19961–19973. [PubMed: 19429677]
57. Sebastian D, Guitart M, Garcia-Martinez C, Mauvezin C, Orellana-Gavalda JM, Serra D, et al. Novel role of FATP1 in mitochondrial fatty acid oxidation in skeletal muscle cells. J Lipid Res. 2009; 50:1789–1799. [PubMed: 19429947]
58. Smithies O, Maeda N. Gene targeting approaches to complex genetic diseases: Atherosclerosis and essential hypertension. Proc Natl Acad Sci USA. 1995; 92:5266–5272. [PubMed: 7777495]
59. Ujihara M, Nakajima K, Yamamoto M, Teraishi M, Uchida Y, Akiyama M, et al. Epidermal triglyceride levels are correlated with severity of ichthyosis in Dorfman-Chanarin syndrome. Journal of dermatological science. 2010; 57:102–107. [PubMed: 20022472]
60. Voss CV, Davies BS, Tat S, Gin P, Fong LG, Pelletier C, et al. Mutations in lipoprotein lipase that block binding to the endothelial cell transporter GPIHBP1. Proc Natl Acad Sci USA. 2011; 108:7980–7984. [PubMed: 21518912]
61. Weinstein MM, Goulbourne CN, Davies BS, Tu Y, Barnes RH 2nd, Watkins SM, et al. Reciprocal metabolic perturbations in the adipose tissue and liver of GPIHBP1-deficient mice. Arterioscler Thromb Vasc Biol. 2012; 32:230–235. [PubMed: 22173228]
62. Weinstein MM, Tu Y, Beigneux AP, Davies BS, Gin P, Voss C, et al. Cholesterol intake modulates plasma triglyceride levels in glycosylphosphatidylinositol HDL-binding protein 1-deficient mice. Arterioscler Thromb Vasc Biol. 2010; 30:2106–2113. [PubMed: 20814015]
63. Weinstein MM, Yin L, Beigneux AP, Davies BS, Gin P, Estrada K, et al. Abnormal patterns of lipoprotein lipase release into the plasma in GPIHBP1-deficient mice. J Biol Chem. 2008; 283:34511–34518. [PubMed: 18845532]
64. Weinstein MM, Yin L, Tu Y, Wang X, Wu X, Castellani LW, et al. Chylomicronemia elicits atherosclerosis in mice. Arterioscler Thromb Vasc Biol. 2010; 30:20–23. [PubMed: 19815815]
65. Wiczer BM, Bernlohr DA. A novel role for fatty acid transport protein 1 in the regulation of tricarboxylic acid cycle and mitochondrial function in 3T3-L1 adipocytes. J Lipid Res. 2009; 50:2502–2513. [PubMed: 19535819]
66. Wilanowski T, Caddy J, Ting SB, Hislop NR, Cerruti L, Auden A, et al. Perturbed desmosomal cadherin expression in grainy head-like 1-null mice. EMBO J. 2008; 27:886–897. [PubMed: 18288204]
67. Xu J, Nicholson BJ. The role of connexins in ear and skin physiology - functional insights from disease-associated mutations. Biochim Biophys Acta. 2013; 1828:167–178. [PubMed: 22796187]

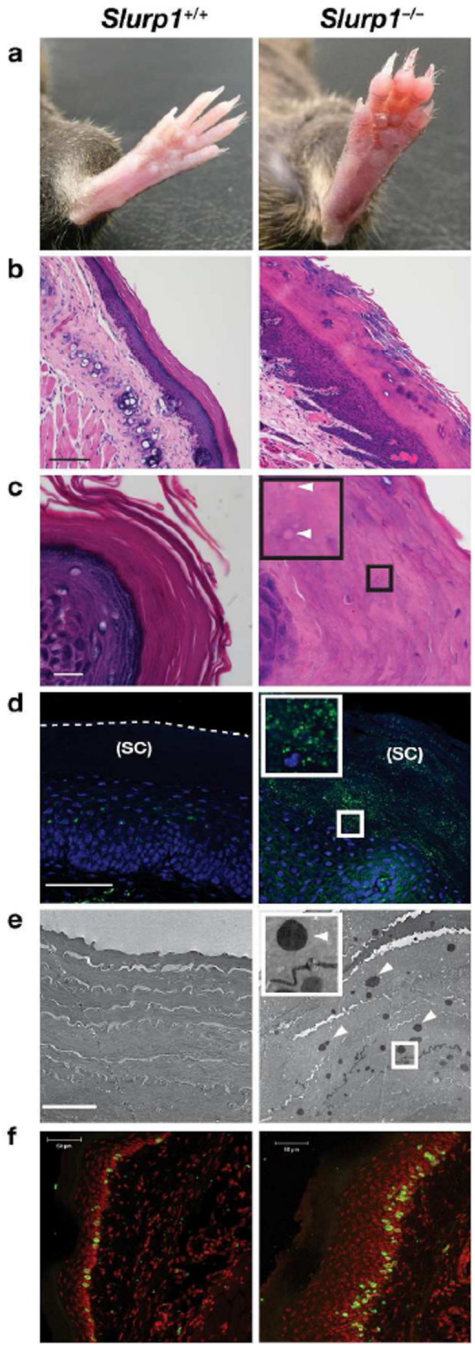

Figure 1. Palmoplantar keratoderma and increased stratum corneum lipid droplets in *Slurp1*$^{-/-}$ mice

(**A**) Paws from wild-type and *Slurp1*$^{-/-}$ mice, revealing markedly thickened skin in *Slurp1*$^{-/-}$ mice. (**B–C**) Hematoxylin and eosin–stained sections revealing a thickened epidermis in the paw skin of a *Slurp1*$^{-/-}$ mouse, along with many tiny lipid droplets in the stratum corneum (arrowheads). Scale bars = 50 μm and 10 μm for B and C respectively. (**D**) BODIPY 493/503 (green) staining showing lipid droplets in the stratum corneum (SC) of the paw skin of a *Slurp1*$^{-/-}$ mouse. DNA is stained with DAPI (blue). Scale bar = 50 μm. (**E**)

Electron micrograph showing lipid droplets in the stratum corneum of *Slurp1*$^{-/-}$ paw skin (arrowheads). Scale bar = 1 μm. (**F**) Increased BrdU incorporation into DNA of paw keratinocytes of *Slurp1*$^{-/-}$ mice (green). DNA is stained with DAPI (red). Scale bar = 50 μm.

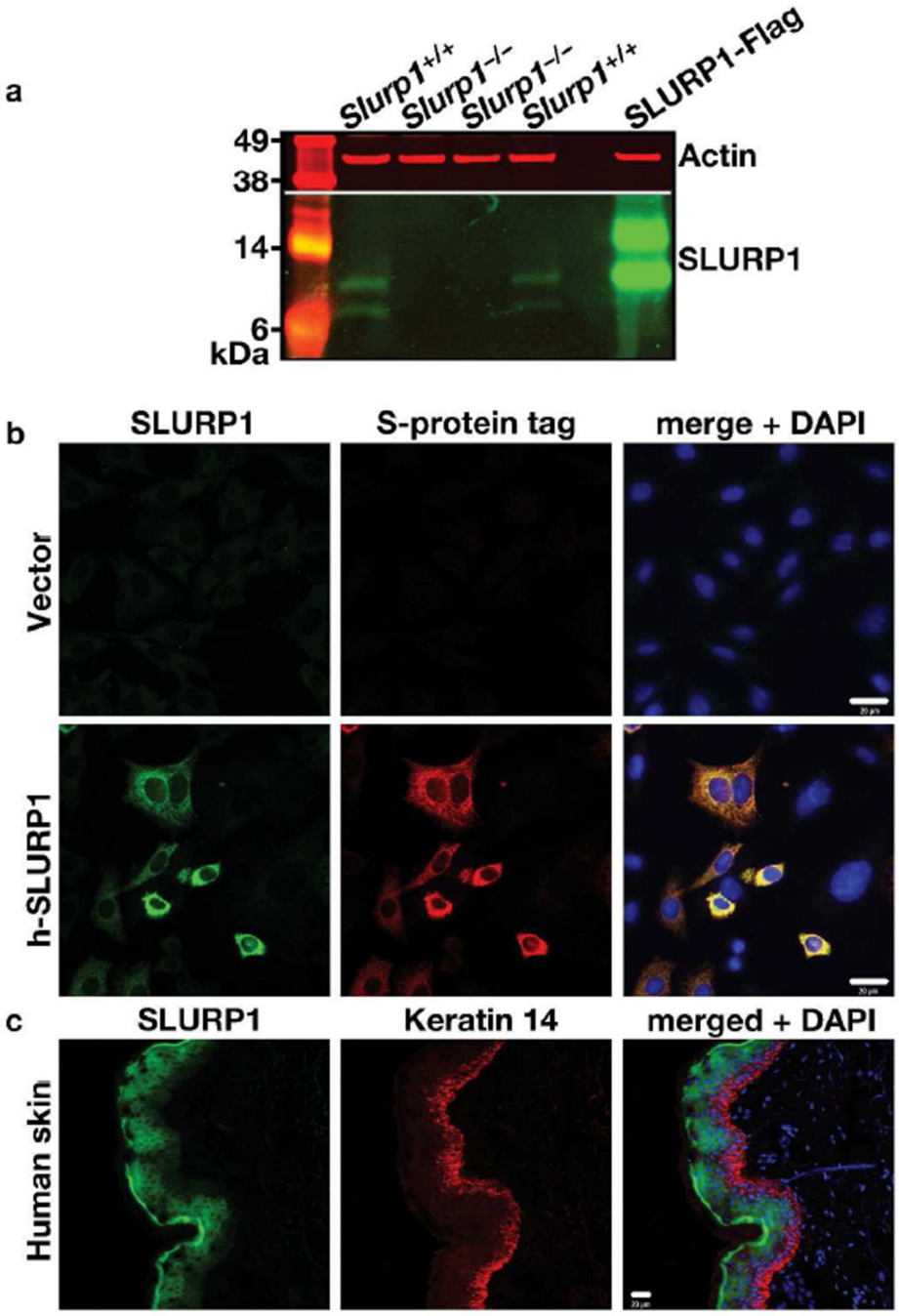

Figure 2. Immunochemical detection of SLURP1

(A) Western blot of extracts of paw skin from wild-type (*Slurp1*$^{+/+}$) and *Slurp1*$^{-/-}$ mice with an antibody against a mouse SLURP1 peptide. CHO cells transfected with a flag-tagged mouse SLURP1 expression vector were used as a control. SLURP1, like nearly all other Ly6 proteins, has an N-linked glycosylation site, and the two SLURP1 bands likely reflect glycosylated and nonglycosylated versions of the protein (Beigneux *et al.*, 2008). The SLURP1 antibody did not cross-react with SLURP2. (**B**) The specificity of the human SLURP1 antibody (green) in these studies was assessed by immunocytochemistry. CHO-K1

cells were transiently transfected with an empty vector or an S-protein–tagged human SLURP1 expression vector. Cells that had been transiently transfected with the S-protein–tagged SLURP1 vector were identified with an S-protein–specific antibody (red). (**C**) Detection of SLURP1 (green) in human skin by immunohistochemistry with a human SLURP1 antibody. Keratin 14 (red) was used as a marker of basal keratinocytes; DNA was stained with DAPI (blue). Scale bars = 20 μm.

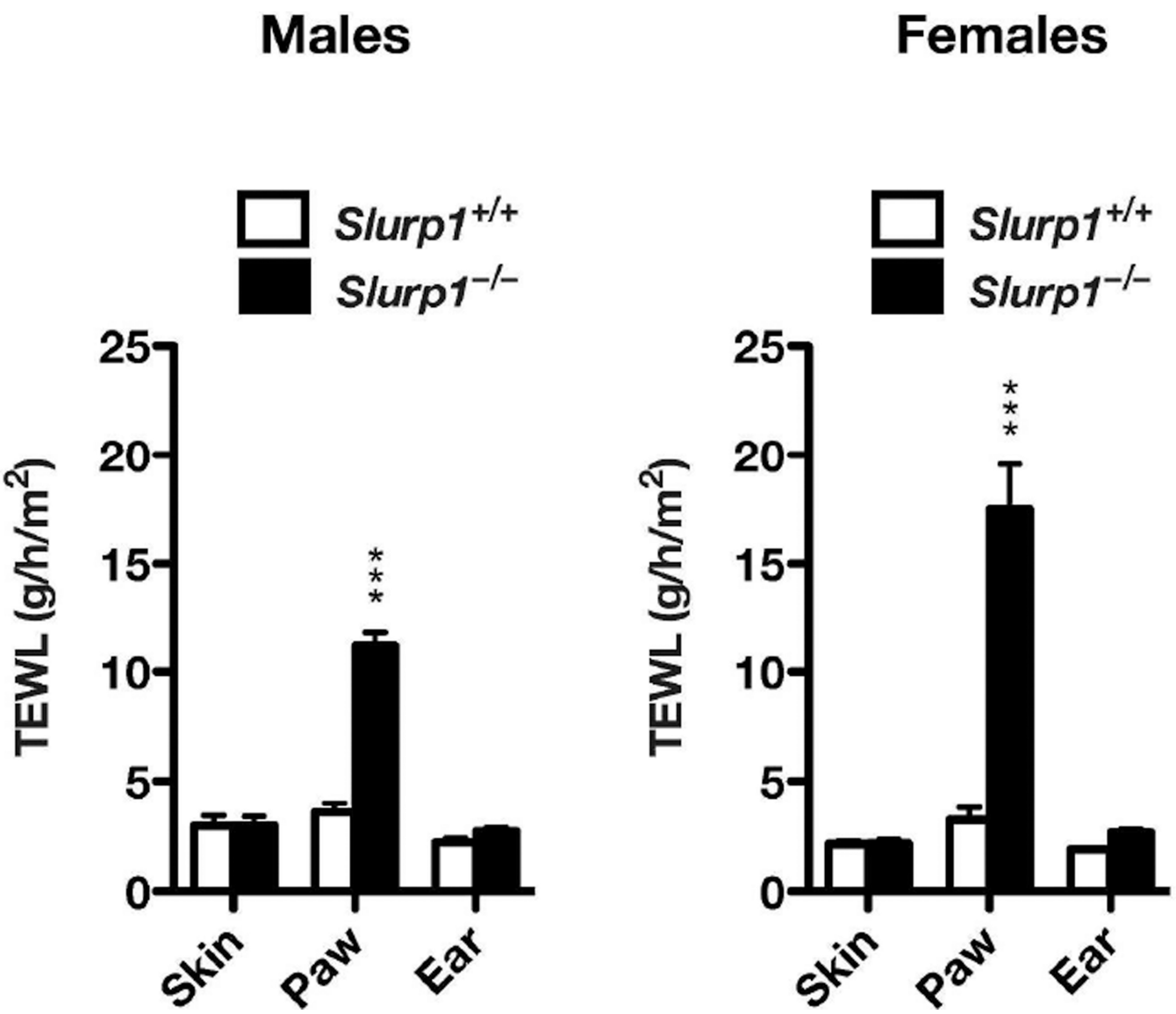

Figure 3. Evaporative water loss from the paw, ear, and back skin of *Slurp1*$^{+/+}$ and *Slurp1*$^{-/-}$ mice

Measurements of evaporative water loss were performed with an RG1 evaporimeter (n = 6/group). TEWL, Transepidermal water loss. *P < 0.05; **P < 0.01; ***P < 0.001.

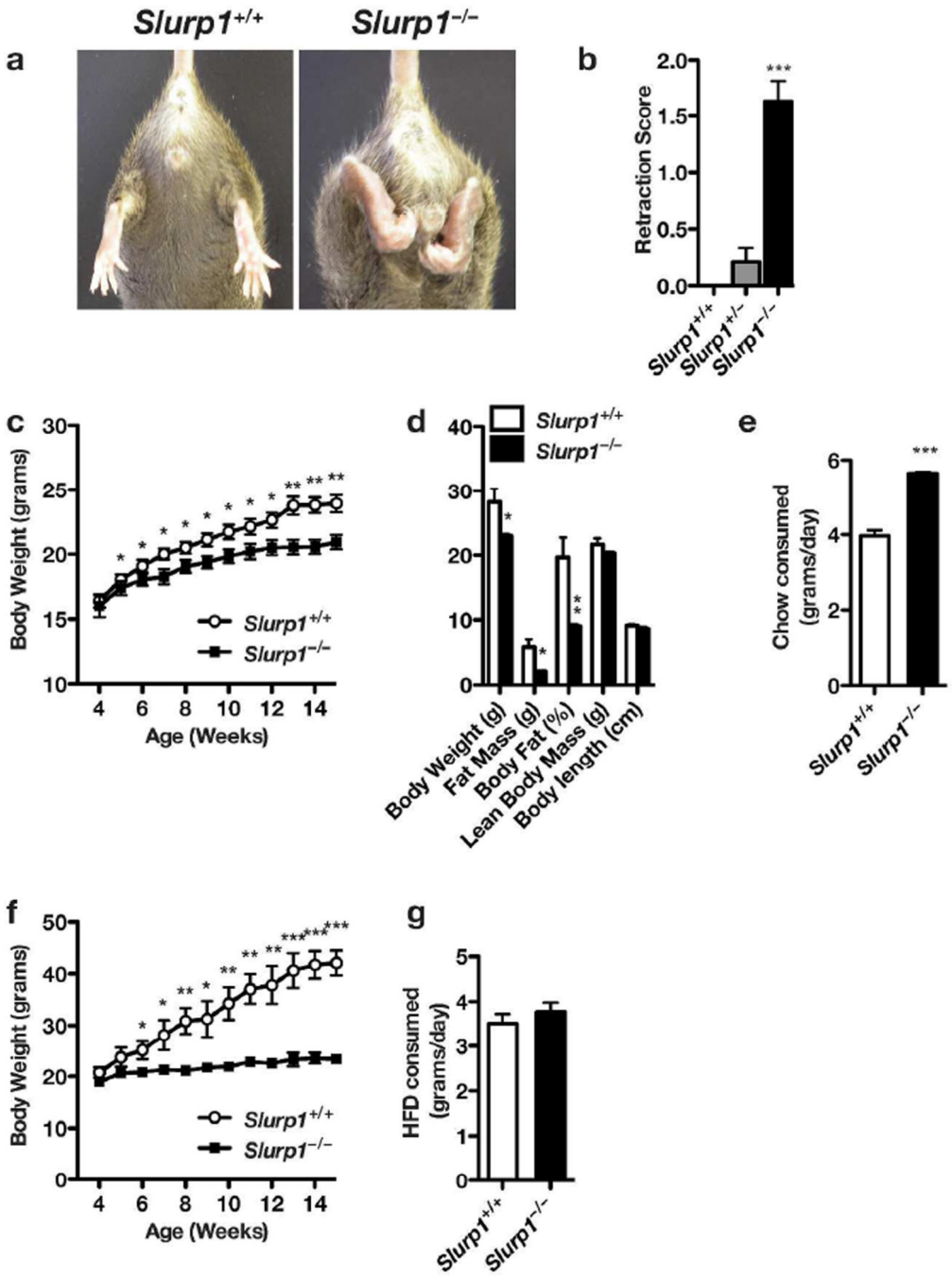

Figure 4. "Non-skin" phenotypes in *Slurp1*$^{-/-}$ mice

(A) Hind limb clasping in male *Slurp1*$^{-/-}$ mice when picked up by the tail (similar results were observed with female *Slurp1*$^{-/-}$ mice). (**B**) Quantification of the hind limb clasping phenotype (0 for no hind-limb retraction, 1 for unilateral retraction, 2 for bilateral retraction) (n = 16 for *Slurp1*$^{+/+}$; n = 19 for *Slurp1*$^{+/-}$; and n = 17 for *Slurp1*$^{-/-}$ mice). ***$P < 0.001$ (*Slurp1*$^{+/+}$ vs. *Slurp1*$^{-/-}$). **(C)** Weight gain in chow-fed female *Slurp1*$^{+/+}$ and *Slurp1*$^{-/-}$ mice (4–15 weeks of age; n = 11/group). Similar results were observed with male mice (**D**) Reduced adiposity in 7-month-old chow-fed female *Slurp1*$^{-/-}$ mice, as judged by NMR (n =

5/group). (**E**) Food consumption in male *Slurp1*$^{+/+}$ and *Slurp1*$^{-/-}$ mice over 24 h. Similar results were observed in two independent experiments (n = 3 mice/group/experiment). (**F**) *Slurp1*$^{-/-}$ mice are resistant to diet-induced obesity. Female *Slurp1*$^{-/-}$ (n = 4) and *Slurp1*$^{+/+}$ mice (n = 3) were fed a high-fat diet for 11 weeks and weight gain was analyzed. Similar results were observed with male mice. *P < 0.05; **P < 0.01; ***P < 0.001. (**G**) Consumption of the high-fat diet (HFD) by *Slurp1*$^{+/+}$ and *Slurp1*$^{-/-}$ mice over 24 h (n = 3/group).

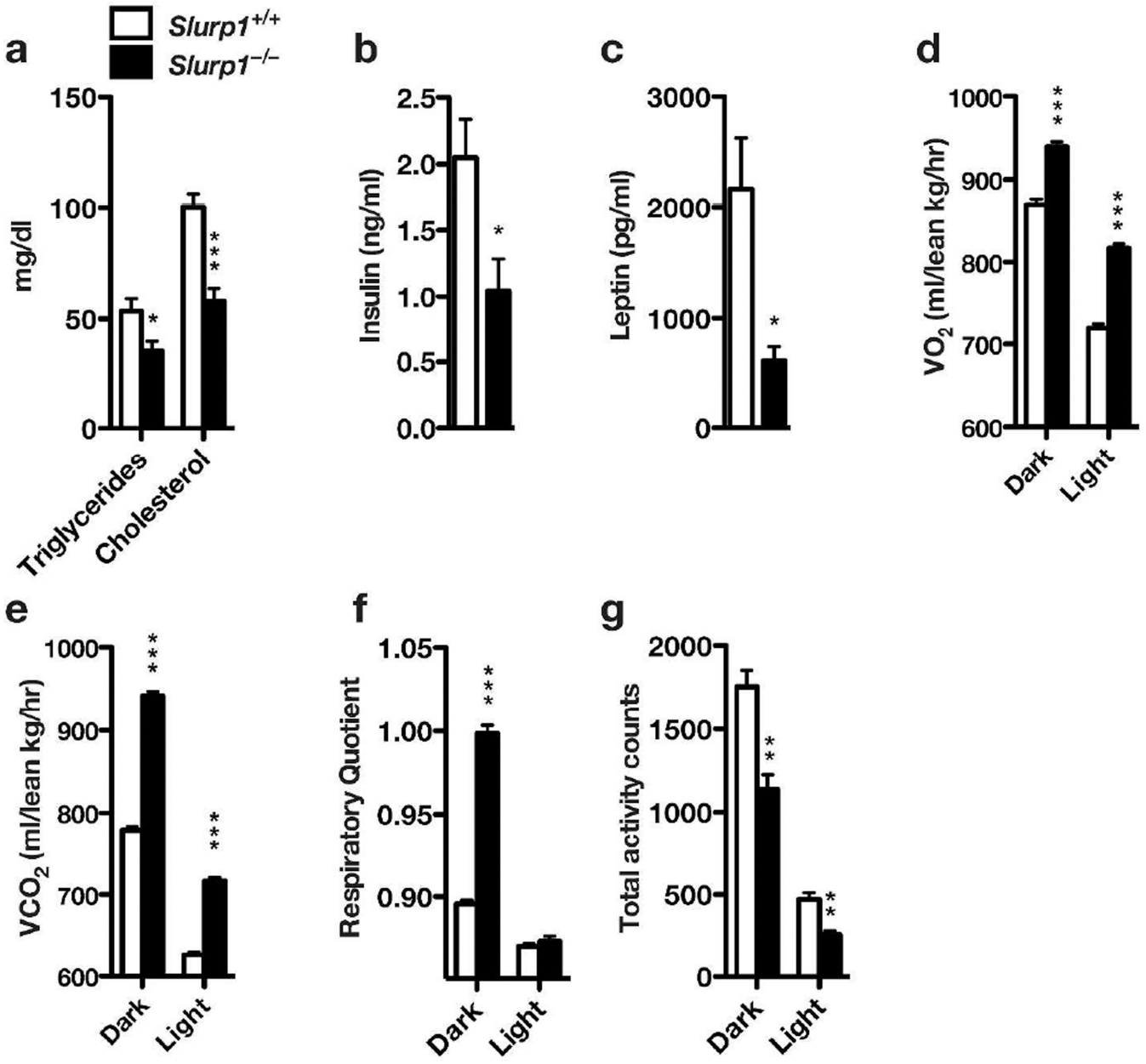

Figure 5. Altered metabolic parameters in *Slurp1*$^{-/-}$ mice

Plasma levels of cholesterol and triglycerides (males, n = 10/group) (**A**), insulin (males, n = 9 wild-type mice; n = 10 *Slurp1*$^{-/-}$ mice) (**B**), and leptin (males, n = 6 wild-type mice; n = 4 *Slurp1*$^{-/-}$ mice) (**C**) in wild-type and *Slurp1*$^{-/-}$ mice. *P < 0.05; **P < 0.01; ***P < 0.001. (**D**) Metabolic cage studies revealing increased oxygen consumption (VO_2) in male *Slurp1*$^{-/-}$ mice. (**E**) CO_2 production. (**F**) Respiratory quotient measurements during two dark and light cycles. (**G**) Decreased activity in male *Slurp1*$^{-/-}$ mice. Bar graph showing total activity (the sum of X Total, X Ambulatory, and Z Total). X Total, total counts of beam interference in the X dimension, including stationary positions; X Ambulatory, multiple beam breaks in the X dimension; Z Total, line breaks in the Z dimension (rearing up) (n = 3/

group). Similar results were observed in two independent experiments. *$P < 0.05$; **$P < 0.01$; ***$P < 0.001$.

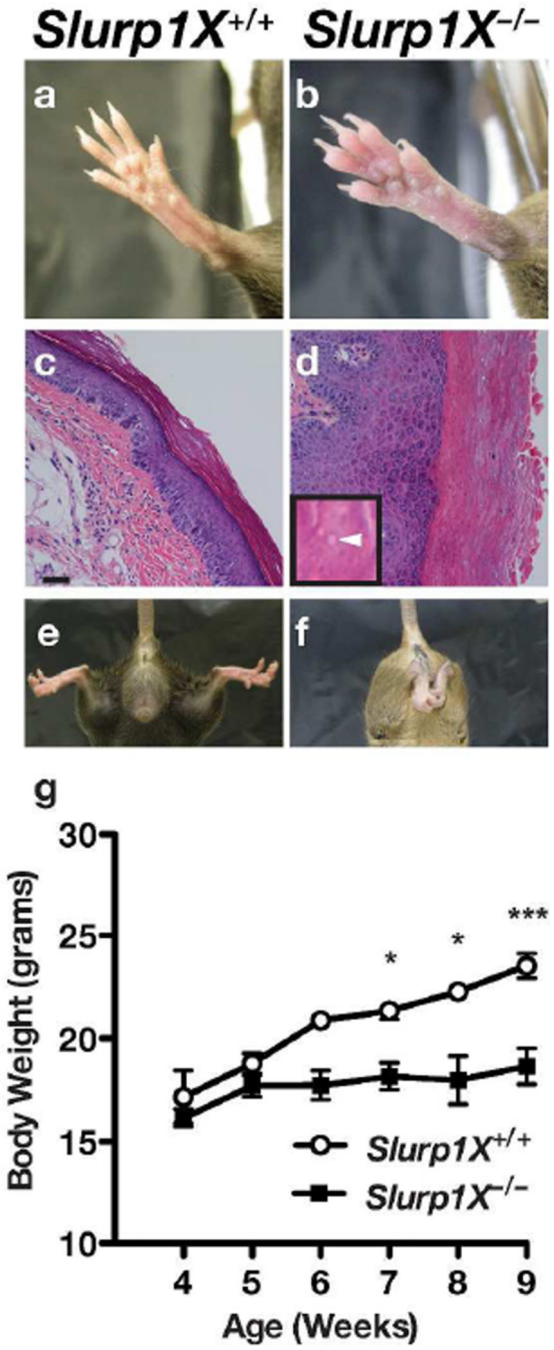

Figure 6. *Slurp1X*$^{-/-}$ mice exhibit PPK and the same "non-skin" disease phenotypes observed in the original line of *Slurp1* knockout mice

(**A–B**) Paws of male *Slurp1X*$^{+/+}$ and *Slurp1X*$^{-/-}$ mice at 12 weeks of age. (**C–D**) Hematoxylin and eosin–stained sections revealing a thickened epidermis in the paw skin of a *Slurp1X*$^{-/-}$ mouse. Higher-powered images revealed many small lipid droplets in the stratum corneum (arrowhead). Scale bar = 50 μm. (**E–F**) Hind limb clasping in a male *Slurp1X*$^{-/-}$ mouse. Similar results were observed with female mice. (**G**) Reduced body weight in *Slurp1X*$^{-/-}$ mice. Serial measurements of body weight revealed a 15–20%

reduction in body weight in 9-week-old *Slurp1X*$^{-/-}$ female mice on chow diet, very similar to findings in the original line of *Slurp1* knockout mice. *$P < 0.05$; ***$P < 0.001$.